EmAIT

EMERGING ADVANCES IN INTEGRATED TECHNOLOGY
e-ISSN: 2773-5540

Vol. 7 No. 1 (2026) 1-14
https://publisher.uthm.edu.my/ojs/index.php/emait

Surface Roughness Investigation of Industrial Robot-Based Milling for UHMWPE: A Parametric Study

Wan Nor Shela Ezwane Wan Jusoh[1]*, Mohamad Irwan Yahaya[1], Shukri Zakaria[1], Mahamad Hisyam Mahamad Basri[1], Razak Daud[2]

[1] *Mechanical Engineering Studies, Universiti Teknologi Mara Cawangan Pulau Pinang, Permatang Pauh Campus, 13500 Permatang Pauh, Pulau Pinang, MALAYSIA*

[2] *Jabatan Kejuruteraan Mekanikal, Politeknik Ibrahim Sultan, 81700 Pasir Gudang, Johor Darul Ta'zim, MALAYSIA*

*Corresponding Author: 2024829196@student.edu.my
DOI: https://doi.org/10.30880/emait.2026.07.01.001

Article Info

Received: 24 April 2026
Accepted: 23 June 2026
Available online: 30 June 2026

Keywords

Robotic machining, UHMWPE, surface roughness, thermoplastic processing, machining parameters

Abstract

This study investigates the surface quality achievable in robotic milling of Ultra-High Molecular Weight Polyethylene (UHMWPE) components using a KUKA KR120 R2700 six-axis industrial robot equipped with a high-speed spindle. While conventional CNC milling of UHMWPE has been extensively studied, the application of industrial robots for this biomedical thermoplastic remains underexplored despite offering superior flexibility and lower capital costs. A parametric investigation was conducted on spindle speed (6500, 12500, 18500 rpm) and feed rates (180, 900, 1620 mm/min) at three levels with a constant depth of cut (2 mm). The surface quality was assessed in terms of arithmetic average roughness (Ra), root mean square roughness (Rq), and maximum peak-to-valley height (Rz), retrieved and measured through contact profilometry, with three measurements for each condition. Findings indicate a range of surface roughness of Ra = 1.29-3.78 µm for the entire range of parameters, with 1.29 µm Ra roughness at 18500 rpm and 1620 mm/min. The two-way interaction effects showed that all main effects and their interaction were significant ($p = 0.0102$.) This indicates that for the required optimal range of surface finishes all factors must be selected in a synergistic manner. The predictive models showed good agreement with experimental results ($R^2 = 0.8668$), indicating satisfactory predictive capability. These findings suggest that robotic systems have the potential to be applied as a flexible alternative to CNC machining in suitable applications. Further investigation is required to evaluate tool wear, material removal rate, and dimensional accuracy for a comprehensive assessment of robotic milling performance.

1. Introduction

Today's manufacturers face the problem of having to achieve and manage operational flexibility, while also needing to meet the demands of high precision work and increased customization [1]. CNC milling machines have been and continue to be the gold standard for the precision engineering of components because of their ability to machine complex components with structural rigidity, accurate control of motion and the capability to produce consistent accuracy and consistent surface finishes with their proven reliability [2, 3]. However, CNCs have been faced with challenges such as expensive machine costs, long set up times, and even longer lead times. This has led to the exploration of lightweight CNC alternatives that can provide the same milling quality at a more affordable cost and with added flexibility [4]. Consequently, industries looking for more adaptable and lighter cost solutions have begun to focus on the use of industrial robots as their preferred machining systems [5].

A number of recent studies identified sustainability and adaptability as primary drivers of broader market adoption within the domain. Specifically, Valente et al. [6] stressed the benefits of recyclability and environmental sustainability, Qiao et al. [7] the importance of cost-effective and lightweight materials, and Periasamy et al. [8] the rapid production rates and potential of aerospace applications. Collectively, these differing patterns of emphasis illustrate target thermoplastic materials serve a range of manufacturing needs simultaneously, namely, environmental sustainability, cost-effective, and adaptable processing. For that reason, they are preferentially positioned across a wider range of industries. However, almost all of this literature is on fiber-reinforced thermoplastic composites, as opposed to pure thermoplastic materials, like UHMWPE, that are widely utilized in biomedical and precision engineering but remain comparatively unstudied in the context of robotic machining.

Among thermoplastic materials, UHMWPE represents a unique case study due to its distinct surface integrity challenges and its widespread use in biomedical and engineering applications. UHMWPE is widely used in bioengineering and biomedical applications due to its excellent wear resistance, low friction coefficient, and biocompatibility. Samad [9] describes UHMWPE as “the tribologist’s polymer,” because of wear resistance, low friction and biocompatibility. These exceptional properties have led to its widespread use in orthopaedic implants, prostheses, and bearing components across multiple industries [10]. Rahman et al. [11] reviewed the clinical use of UHMWPE in artificial joint prostheses since the 1960s, reporting that the material has remained biocompatible and has performed reliably over several decades. Bistolfi et al. [12] further affirm that UHMWPE remains the primary bearing material in modern hip and knee arthroplasty applications. Considering the long-term use of UHMWPE in load-bearing applications, surface quality is of foremost importance. Surface roughness plays a critical role in tribological performance, as it directly influences wear rate and reduces the longevity of biomedical implants [13]. Consequently, CNC milling of UHMWPE has been extensively investigated to establish process parameters yielding medical-grade surface finishes. Lestari et al. [14] demonstrated that optimized milling parameters significantly improve surface smoothness and reduce wear in UHMWPE components. This was further validated by Piska and Urbancova [15], who showed that advanced machining approaches are required to develop surfaces that meet critical specifications within the clinical field.

Six-axis industrial robots equipped with high-speed spindles can perform milling operations comparable to CNC machines while offering larger workspaces, greater flexibility, and easier integration into automated production systems [16]. Their reconfigurability makes them particularly attractive for small-batch or customized manufacturing, where frequent product changes and varying part geometries are common. Asif et al. [17] demonstrated that reconfigurable manufacturing systems provide the modularity and integrability necessary for rapid adaptation to new product variants. However, industrial robots were not originally designed as high-stiffness machine tools. Their serial kinematic structure and articulated joints result in lower rigidity and higher compliance under cutting loads compared to dedicated CNC machines [18]. Consequently, concerns remain regarding their ability to consistently achieve the surface quality required for precision UHMWPE components, particularly under practical cutting parameter ranges [19].

UHMWPE has low thermal conductivity, is highly ductile, and exhibits viscoelastic behavior that makes it difficult to machine. Hu et al. [20] showed that the cutting mechanism is dominated by ductile fracture and elastic retraction; however, when the cutting parameters are improperly selected, poor finish with smeared surfaces, burrs, chip welds, thermally degraded areas, and poor surface finish are produced [21]. Other than limited work, scholarship on UHMWPE has predominantly addressed CNC machining. Research has consistently demonstrated that spindle speed, feed rate, and step-over govern surface roughness, with feed rate emerging as the dominant factor [14], [22]. Machining parameters indirectly influence wear behavior through their effect on surface finish, as shown by Lestari et al. [23]. However, Piska and Urbancova [15] noted that the thermal and viscoelastic properties of UHMWPE material pose significant challenges with respect to machining parameters in order to obtain good surface finish and quality, so parameter selection is therefore non-trivial and requires careful optimization. Despite extensive research on CNC machining, the application of industrial robots for milling UHMWPE remains underexplored.

The extent of surface roughness achieved with robotic systems continues to be explored, but quantification remains limited across a practical range of processing parameters. Schmidt et al. provide a notable example of recent robot-based machining research, which largely emphasizes metallic and composite workpiece materials, while prioritizing stiffness modelling, pose optimization, and control hierarchy [24]. Although studies such as these are illustrative of the general state of robotic machining, the findings are not directly applicable to UHMWPE, as this material differs vastly in its deformation response and thermal properties [25]. Therefore, experimental studies must be conducted to validate the claims made in the literature. Table 1 compiles existing studies on the machining of UHMWPE and related polymers, highlighting the near absence of robotic systems applied to this material class. While previous studies have established surface roughness benchmarks for CNC machining of UHMWPE, a direct evaluation of how robotic milling compares to these established ranges remains limited. Therefore, this study not only investigates parametric effects but also positions the obtained results relative to CNC-based benchmarks to assess feasibility.

The aim of this study is to evaluate the surface quality achievable through robotic milling of UHMWPE and to assess its feasibility for practical manufacturing applications. Since surface finish is a fundamental requirement for UHMWPE components, this work first focuses on establishing whether acceptable surface roughness can be achieved before considering broader performance criteria such as tool wear, dimensional accuracy, and productivity. An experimental approach was adopted, in which UHMWPE specimens were machined using a six-axis industrial robot. The effects of spindle speed and feed rate on surface roughness were investigated while maintaining a constant depth of cut, with roughness quantified using a contact profilometer. By analyzing surface roughness trends across the tested parameter combinations, this study identifies machining conditions that yield finishes consistent with the requirements of UHMWPE applications. The contribution of this work lies in providing quantitative experimental evidence on the surface quality achievable in robotic milling of UHMWPE, as well as defining a practical parameter window within which acceptable surface finish can be attained. These findings establish an initial basis for evaluating industrial robots as a flexible machining alternative for UHMWPE component manufacturing.

A holistic feasibility evaluation would require consideration of factors such as material removal rates, tool life, and economic aspects. However, the present study focuses specifically on surface quality, as it represents a primary feasibility criterion for UHMWPE machining applications. Other important factors, including tool wear, dimensional accuracy, and productivity, are beyond the scope of this work and are identified as directions for future investigation. If acceptable surface finish cannot be achieved, the practical suitability of robotic systems for UHMWPE machining would remain limited regardless of other potential advantages. Accordingly, this study investigates the surface roughness response to variations in spindle speed and feed rate, thereby providing experimental data to support future, more comprehensive feasibility assessments.

Table 1 *Summary of recent machining studies on UHMWPE and engineering polymers, highlighting the research gap in robotic milling applications*

Study	Platform	Material	Cutting Parameters	Surface Roughness Achieved	Optimization Method	Key Findings / Limitations
Basuki & Ismail, 2018 [22]	CNC Milling	UHMWPE	Cutting speed: 150 m/min (constant); Feed rate: 0.025–0.2 mm/rev Depth of cut: 0.05–0.2 mm	Ra < 2 µm	Multiple Regression + ANOVA	Feed rate is the most significant factor
W.D. Lestari et al., 2019 [23]	CNC Milling (3-axis)	UHMWPE	Spindle speed: 6500–7500 rpm; Feed rate: 1000–2000 mm/rev; Step over: 0.01–0.1 mm	Minimum Ra: ~0.577 µm	Taguchi, (RSM)	Spindle speed was the most influential factor
Piska et al. (2022) [15]	CNC machining center (3-axis)	UHMWPE	Speed: 8,000–12,000 rpm; Feed: 400–800 mm/min; Depth: 0.2–0.5 mm	*Ra* = 0.8–2.1 µm; *Rq* = 1.0–2.6 µm; *Rz* = 4.2–8.5 µm	Taguchi DOE	CNC baseline for UHMWPE; emphasized toolpath strategy
Wambua et al. (2022) [26]	CNC milling (3-axis)	PMMA	Speed: 6,000–14,000 rpm; Feed: 500–1,000 mm/min; Depth: 0.15–0.3 mm	*Ra*=0.92–2.34 µm; *Rq* = 1.15–2.87 µm	Taguchi L9 orthogonal array	Spindle speed dominant; CNC-specific optimization

Study	Platform	Material	Cutting Parameters	Surface Roughness Achieved	Optimization Method	Key Findings / Limitations
Beşliu-Băncescu et al. (2024) [27]	CNC milling (5-axis)	PEEK	Speed: 8,000–16,000 rpm; Feed: 400–1,000 mm/min; Depth: 0.15–0.35 mm	*Ra* = 1.1–2.9 µm; *Rz* = 5.8–12.4 µm	Full factorial DOE	Machining strategy influenced quality; CNC platform only
Present Study (2026)	Robotic milling (6-axis KUKA KR120 R2700)	UHMWPE	Speed: 6500–18500 rpm; Feed: 180–1620 mm/min; Depth: 2 mm (constant)	Ra=1.29-3.78 µm Rq=1.60-4.08 µm Rz=8.10-17.02 µm	Full factorial RSM	Parametric study for UHMWPE

2. Material and Method

2.1 Material Selection and Experimental Configuration

Ultra-high-molecular-weight polyethylene (UHMWPE) was selected as the workpiece material based on its superior machinability characteristics, high impact resistance, low coefficient of friction, and biocompatibility properties that have established it as a critical thermoplastic in both engineering and biomedical applications [28]. Specimen blanks were prepared as rectangular blocks with dimensions of 50 mm × 50 mm × 50 mm, providing a flat milling surface area of 50 mm × 10 mm oriented perpendicular to the tool axis. The thermomechanical properties of the UHMWPE material employed in this investigation are summarized in Table 2.

All machining operations were conducted using a KUKA KR120 R2700 six-axis industrial robot with 120 kg payload capacity and 2700 mm operational reach. At the end effector of the robot was a high-speed spindle motor, capable of reaching a speed of 24000 rpm, which allowed it to fully control the tool path. Thus, the setup provided the system with six degrees of freedom, allowing flexible and adaptive motion control during the milling operation. A 10 mm diameter two-flute High Speed Steel (HSS) end mill served as the cutting tool, selected for its suitability in thermoplastic machining and consistent flat-face milling capability. The robotic milling process employed a down-milling strategy to enhance surface quality by reducing chip adhesion and heat generation in polymeric materials. A custom fixture was designed to rigidly secure UHMWPE specimens to the robot base platform. This minimized compliance-induced vibrations and prevented workpiece displacement during machining. The complete experimental configuration, including robotic manipulator, spindle assembly, and fixture system, is illustrated in Fig. 1.

Table 2 *UHMWPE material properties used in the experiment*

Properties	Value
Density, g/cm^3	0.93
Yield Stress (MPa)	20
Tensile Modulus of Elasticity (MPa)	680
Melting Temperature (°C)	135
Heat Deflection Temperature (°C)	79
Coefficient of Thermal Expansion	150-230
Dielectric Strength (kV/mm)	45

Emerging Advances in Integrated Technology Vol. 7 No. 1 (2026) p. 1-14

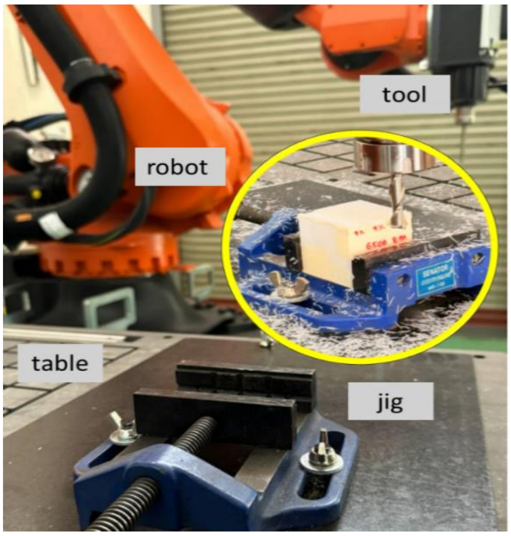

Fig. 1 *Experimental setup for robotic milling [29]*

2.2 Machining Parameter

The variable machining parameters in this research are feed rate and spindle speed as listed in Table 3 while the depth of cut is constant at 2 mm. The selected range of parameters is based on the soft work material, which is non-metal and high-speed steel end mil, according to the machining handbook such as the use of 2-flute for plastic-type materials. The control parameters of work piece size, tool size, and cutting path, on the other hand, must be constant, as described in Table 4, and the parallel path is depicted in Fig. 2.

Table 3 *The range of cutting parameter*

Factor	Symbol	Unit	Low (−1)	Center (0)	High (+1)
Spindle Speed	A	rpm	6500	12500	18500
Feed Rate	B	mm/min	180	900	1620

Table 4 *The machining control parameter*

Type of parameter	Value/control parameter
Cutting tool size	2-flutes, 10 mm diameter HSS
Milling strategy	Parallel
Milled mode	Climb
Cutting condition	Dry

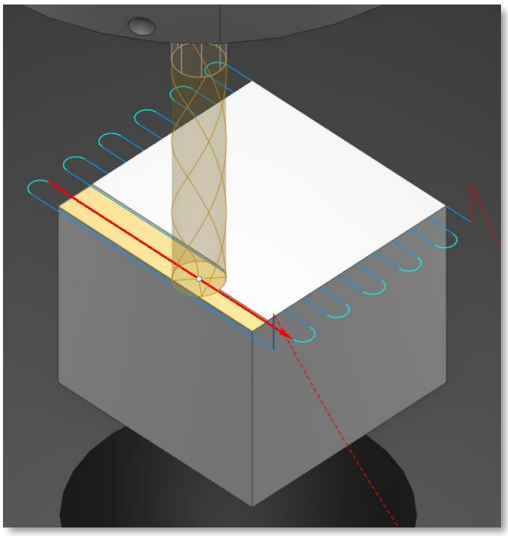

Fig. 2 *A parallel cutting path for face mill operation [30]*

2.3 Experiment Design Matrix

The 9-run matrix was generated using Design-Expert® software (Version 13, Stat-Ease Inc., Minneapolis, MN, USA). The design includes 2 factors and 3 levels. Run order as shown in Table 5. Each factor combination was executed once, with surface roughness measured at three locations per specimen to quantify within-sample variability. Although full experimental replication was not performed, the present work was designed as an initial parametric study to identify preliminary trends in robotic milling of UHMWPE. The three measurement points on each machined surface were used to improve measurement reliability and reduce the influence of local surface variation. This approach provides a practical baseline for assessing the feasibility of robot-based milling as an alternative to conventional CNC machining, while more extensive replicated experiments will be considered in future work.

Table 5 *The list of experimental work consists of different combinations of cutting parameter*

Run	A: Spindle Speed (rpm)	B: Feed Rate (mm/min)	C: Depth of Cut (mm)
1	6500	180	2
2	6500	900	2
3	6500	1620	2
4	12500	180	2
5	12500	900	2
6	12500	1620	2
7	18500	180	2
8	18500	900	2
9	18500	1620	2

3. Result and Discussion

Surface roughness measurements from robotic milling of UHMWPE under 9 Full Factorial design parameter combinations as shown in Table 6. The results show that the machining conditions achieved 1.29 - 3.78 µm for Ra and confirmed significant sensitivity to spindle speed and feed rate with constant depth of cut interaction. Similar variability was observed for Rq (1.60 - 4.08 µm) and Rz (8.10 - 17.02 µm) across the experimental design space.

The surface quality achieved through robotic milling was evaluated against CNC machining benchmarks reported in Table 1. Previous CNC-based studies on UHMWPE have typically reported Ra values below 2 µm under optimized conditions. Although the robotic milling process in this study does not consistently reach the lowest CNC-level roughness, its minimum achieved surface quality is comparable to those reported under certain CNC machining conditions. This indicates that robotic milling can approach functional surface quality requirements, particularly under high spindle speed and feed rate combinations.

Emerging Advances in Integrated Technology Vol. 7 No. 1 (2026) p. 1-14

Table 6 *Results of experiments on surface roughness in UHMWPE*

Run	A: Spindle Speed (rpm)	B: Feed Rate (mm/min)	C: Depth of Cut (mm)	Surface Roughness measurements on the surfaces at each experiment		
				Ra Average (µm)	Rq Average (µm)	Rz Average (µm)
1.	6500	180	2	2.705	3.426	16.622
2.	6500	900	2	3.172	3.934	16.650
3.	6500	1620	2	3.337	3.921	15.120
4.	12500	180	2	3.784	4.578	19.326
5.	12500	900	2	2.372	2.959	14.294
6.	12500	1620	2	2.587	3.187	14.685
7.	18500	180	2	3.438	4.081	17.020
8.	18500	900	2	2.378	2.949	13.272
9.	18500	1620	2	1.294	1.604	8.103

The experimental results reveal a substantial variation in surface roughness across the tested parameter space, with Ra values ranging from 1.29 to 3.78 µm. The lowest surface roughness of Ra = 1.29 µm was achieved at the highest spindle speed (18500 rpm) combined with the highest feed rate (1620 mm/min), while the roughest surface (Ra = 3.78 µm) occurred at moderate spindle speed (12500 rpm) with the lowest feed rate (180 mm/min). These results indicate a non-linear relationship between machining parameters and surface quality, requiring further statistical interpretation.

3.1 Analysis of Variance (ANOVA) and Statistical Significance

The impact of the machining parameters on the surface roughness responses were measured using the two-way interaction of the ANOVA tables. The results of the ANOVA for the surface roughness parameters Ra, Rq and Rz, including the F-values and p-values, were obtained and assessed. These results were then modelled and collated to evaluate the parameters of the machining model. ANOVA results have been summarised in Table 7.

Table 7 *Anova for surface roughness*

Source	Sum of Squares	df	Mean Square	F-value	p-value	Remarks
(a) Average Roughness, Ra						
Model	3.89	3	1.3	10.85	0.0125	significant
A–Spindle Speed	0.7378	1	0.7378	6.18	0.0555	
B–Feed Rate	1.22	1	1.22	10.24	0.024	
AB	1.93	1	1.93	16.13	0.0102	
Residual	0.5971	5	0.1194			
R-squared	0.8668					
Adj R-squared	0.787					
Pred R-squared	0.6567					
Adeq precision	9.9438					
(b) Root Mean Square Roughness, Rq						
Model	5.27	3	1.76	10.92	0.0124	significant
A–Spindle Speed	1.17	1	1.17	7.26	0.0431	
B–Feed Rate	1.9	1	1.9	11.78	0.0186	
AB	2.21	1	2.21	13.72	0.0139	
Residual	0.805	5	0.161			
R-squared	0.8676					
Adj R-squared	0.7881					
Pred R-squared	0.614					
Adeq precision	9.7607					

(c) Maximum Peak-to-Valley Height, Rz						
Model	68.2	3	22.73	10.23	0.0142	significant
A–Spindle Speed	16.66	1	16.66	7.5	0.0409	
B–Feed Rate	37.8	1	37.8	17.01	0.0091	
AB	13.74	1	13.74	6.18	0.0554	
Residual	11.11	5	2.22			
R-squared	0.8599					
Adj R-squared	0.7759					
Pred R-squared	0.452					
Adeq precision	8.7819					

Considering Ra, there is evidence of a major interaction effect (AB: F = 16.13, $p = 0.0102$). This shows that spindle speed and feed rate do not work alone, as they work together to affect surface finish. Feed rate is a main effect (F = 10.24, $p = 0.0240$) and spindle speed effects of minimal importance (F = 6.18, $p = 0.0555$). This is also true of Rq, where all terms of the model achieve significance ($p < 0.05$). This interaction effect is also large, and $p = 0.0139$ confirms the coupled nature of influence of the parameters. Since both speeds ($p = 0.0431$) and feed rates ($p = 0.0186$) affect Rq, it is likely that Rq is the more responsive indicator, and the effects of all parameters are more likely to be captured than in Ra. Regarding the maximum peak to valley height, Rz shows the greatest effect to the variation of feed rate (F = 17.01, $p = 0.0091$) and spindle speeds (F = 7.5, $p = 0.0409$). There effects show borderline significance (F = 6.18, $p = 0.0554$) but some evidence of coupled variation exists.

Across the board, the three models exhibited R^2 scores over the benchmark score of 0.85, precisely measuring surface roughness variations at 86-87%. The robustness of the models is reflected in the adjusted R^2 scores of 0.776-0.788. The accuracy of the precision ratios spanning from 8.78 to 9.94 also suggests that the adjusted values are indeed accurate given that those scores are far above the minimum score of 4.0, indicating that there is a strong connection between variables in the design space. Across each response, the predicted R^2 values tell a different story as there appears to be a varied degree of predictability in the values. While the reasonable differences between adjusted and predicted R^2 values paired Ra and Rq (0.6567 and 0.614, respectively), the adjustments indicate that there is a larger gap in Rz (0.7759) than what the predicted R^2 shows (0.452). Rz is indeed the most complex, likely due to the obscured variabilities concerning the peak-valley metrics, as well as the subtle non-linearities which cannot be predicted as a result of the two-factor interaction. The losses or residual mean square errors (Ra: 0.1194 μm^2, Rq: 0.161 μm^2, Rz: 2.22 μm^2) do indicate that the models behaved adequately and aligned well with the values measured given the response magnitudes significantly larger than those from the residuals. The residuals also have random distribution, thus supporting the initial assumptions made for model fitting.

3.2 Predictive Regression Models

Based on the statistically significant terms identified through ANOVA, predictive regression equations were developed for each surface roughness response using actual machining parameter values. The two-factor interaction models are expressed as:

$$Ra = 2.27280 + 0.000086SS + 0.001381FR - 1.60648E\text{-}07SS \times FR \quad (1)$$

$$Rq = 3.09121 + 0.000081SS + 0.001369FR - 1.72029E\text{-}07SS \times FR \quad (2)$$

$$Rz = 16.79190 + 0.000108SS + 0.001877FR - 4.29070E\text{-}07SS \times FR \quad (3)$$

where SS represents spindle speed (rpm), FR represents feed rate (mm/min), and SS × FR denotes the interaction between spindle speed and feed rate.

The regression models indicate that the surface roughness responses are influenced by both the main effects of spindle speed and feed rate, as well as by their interaction. These models enable the prediction of surface roughness within the investigated experimental domain and provide a quantitative basis for preliminary parameter selection, thereby reducing the need for additional trial-and-error experiments within the tested range. The models are applicable to robotic milling of UHMWPE at a fixed depth of cut of 2 mm and are limited to the parameter ranges examined in this study.

Emerging Advances in Integrated Technology Vol. 7 No. 1 (2026) p. 1-14

3.3 Model Adequacy and Residual Analysis

Model assumptions were verified through residual diagnostic plots shown in Figs. 3-5. Normal probability plots for Ra, Rq, and Rz demonstrate that residuals approximate normal distribution reasonably well, with most data points aligning along the theoretical line. Minor deviations at distribution extremes are expected given the limited sample size (n = 9) and remain within acceptable bounds. Residual-versus-run plots confirm random scatter without systematic patterns or trends across the experimental sequence. All externally studentized residuals fall within ±3 standard deviation limits (indicated by red bounds), with no outliers detected. This validates homoscedasticity assumptions and confirms the absence of lurking variables or time-dependent effects during experimentation. The diagnostic assessment supports model reliability for prediction within the tested parameter space.

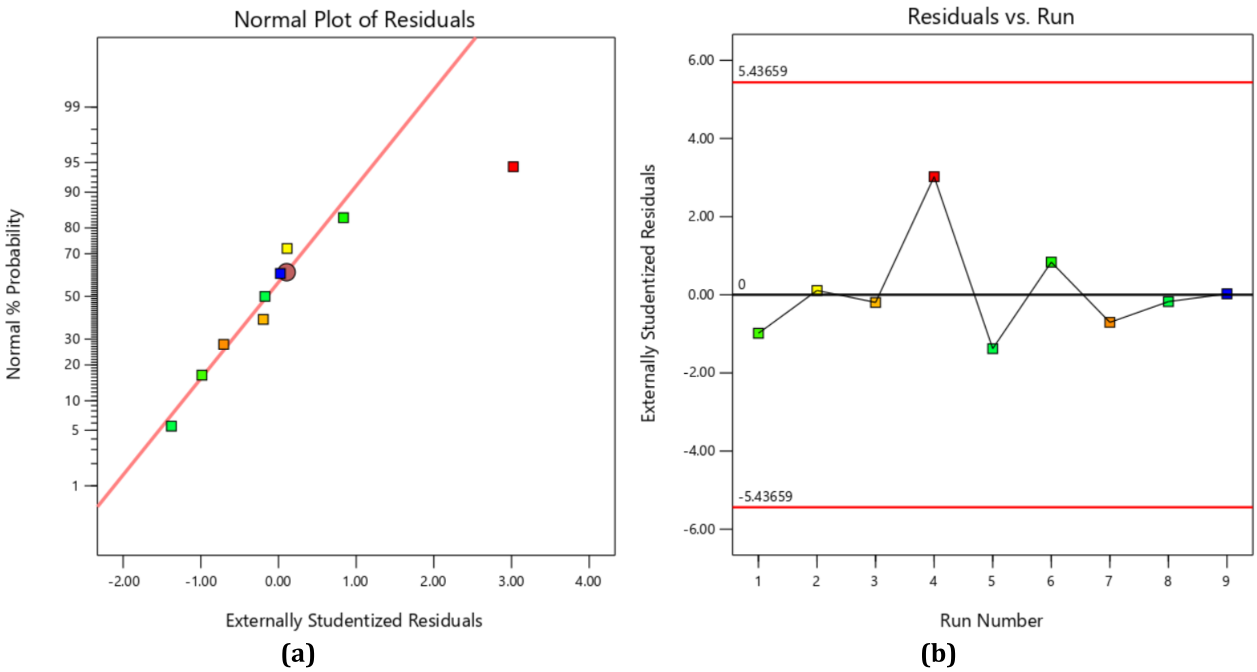

Fig. 3 *Diagnostic plots for Ra: (a) Normal plot of residuals (b) residuals vs. run*

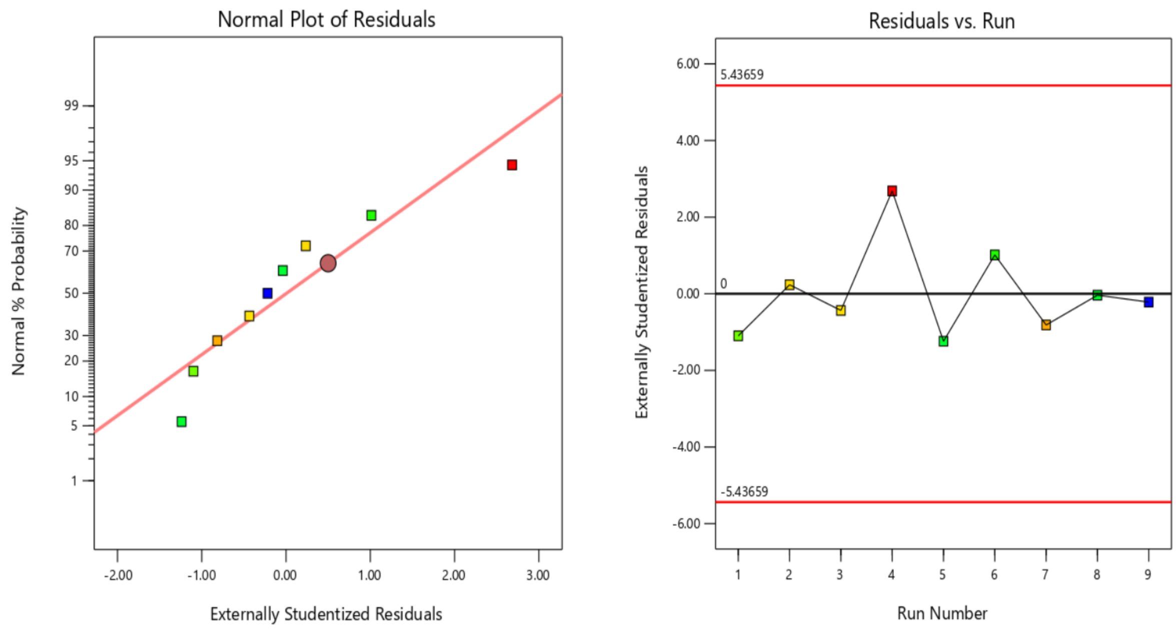

(a) **(b)**

Fig. 4 *Diagnostic plots for Rq: (a) Normal plot of residuals (b) residuals vs. run*

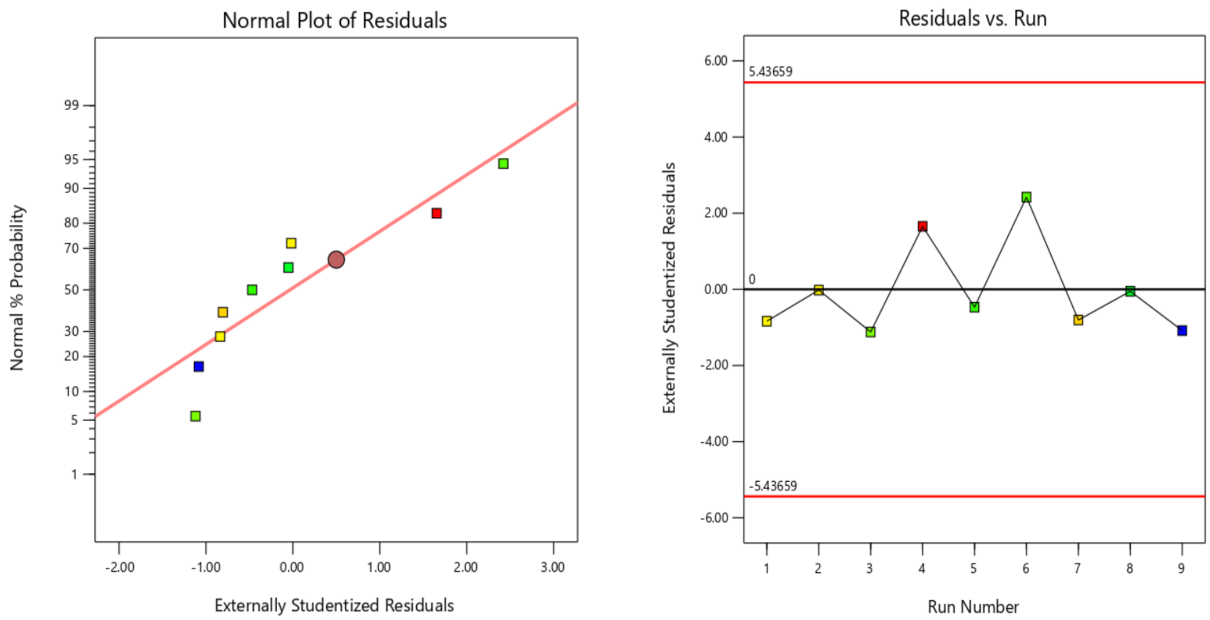

(a) **(b)**

Fig. 5 *Diagnostic plots for Rz: (a) Normal plot of residuals (b) residuals vs. run*

3.4 Response Surface Analysis

Figs. 6-8 contain three-dimensional response surface graphs that show how surface roughness changes across the domains of the feed rate and spindle speed. The response surface of arithmetic average roughness, Ra (Fig. 6), shows a distinct saddle-shaped surface, having minimum value regions at the corner of high spindle speed and high feed rate. With increasingly lower values of spindle speed and feed rate, surface roughness increases. This also shows surface trend along the spindle speed direction, suggesting that the values of roughness in the surface regions lower along the spindle speed direction. The curvature confirms a strong AB interaction term in the ANOVA, demonstrating how parameter effects are coupled instead of being added together, evident by the sharp drop in the saddle surface. The root mean square roughness, Rq, which is also shown in Fig. 7, has the same topological features, sharing the same minimum zone located at maximum values of parameters.

The curvature is similar to Ra, although it appears to be more sensitive to the changes in the feed rate. Longer contour lines along the spindle speed axis support this difference, and these are the same changes that are seen in the ANOVA, which indicate the feed rate value to be more significant for Rq (F=11.78) than it was for Ra (F=10.24). Overall, Rz (Fig. 8) shows the greatest surface curvature, both positively and negatively, and thus the greatest absolute variability (approximately 8 to 20 µm). The top section, as was the case with Ra and Rq, is the same, although the surface displays more abrupt changes in elevation between low and high roughness patches. The projection of the contour shows that the closer spacing is with decreased parameter values, and this indicates that the surface quality is more rapidly degraded when moving from the optimal condition.

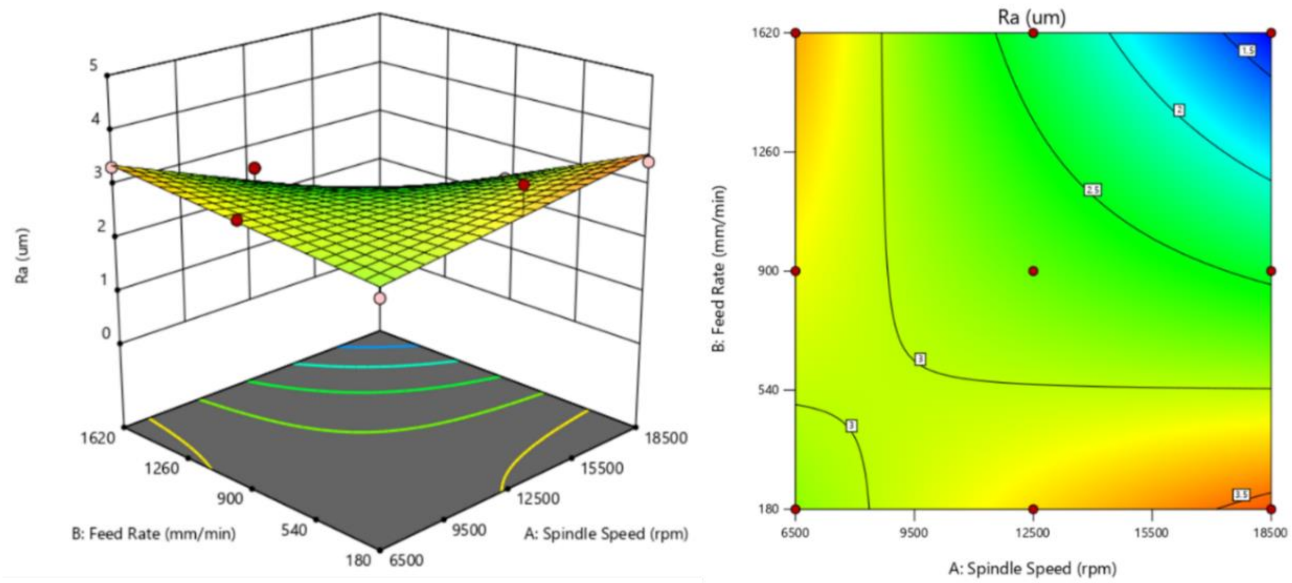

(a) **(b)**

Fig. 6 *Spindle speed versus feed rate: (a) Ra 3-D surface plot; (b) Ra contour plot*

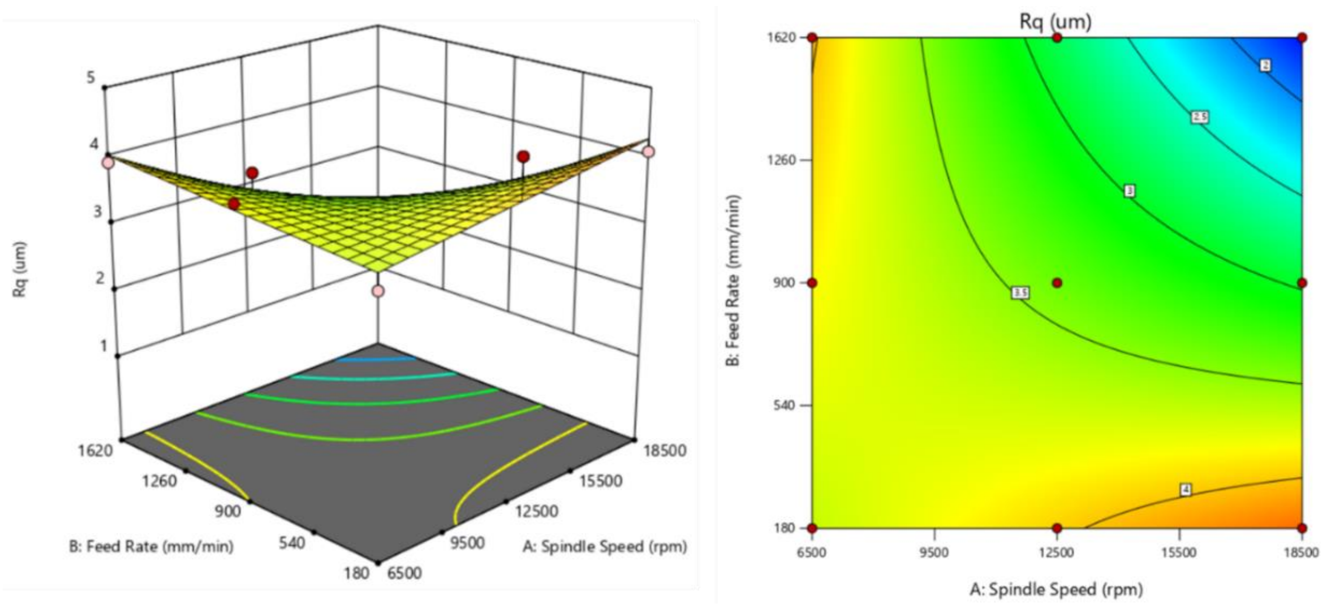

(a) **(b)**

Fig. 7 *Spindle speed versus feed rate: (a) Rq 3-D surface plot; (b) Rq contour plot*

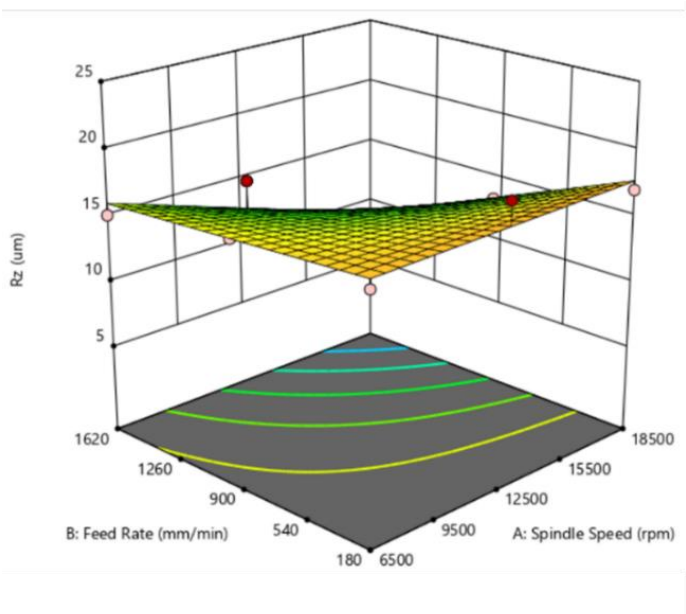

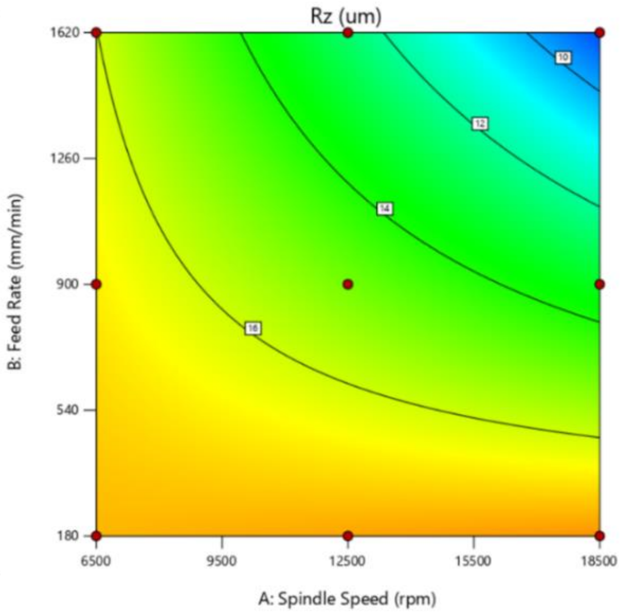

Fig. 8 *Spindle speed versus feed rate: (a) Rz 3-D surface plot; (b) Rz contour plot*

Across all three responses, locating roughness minimums at simultaneous maximum levels of both parameters confirms the synergistic nature of both the spindle speed and feed rate effects. The lack of saddle points and local minima within the design space reflects continuous improvement toward higher parameter values, implying that superior surface finish is possibly achievable when applying more aggressive cutting conditions in UHMWPE robotic milling.

4. Conclusion

This study evaluated the surface quality achievable in robotic milling of UHMWPE components using a KUKA KR120 R2700 industrial robotic platform. Based on an empirical investigation of the interaction between spindle speed and feed rate, surface roughness values (Ra) ranging from 1.29 to 3.78 μm were obtained under the tested conditions, with the minimum roughness achieved at 18500 rpm and a feed rate of 1620 mm/min. These values fall within the range reported for certain medical-grade UHMWPE components.

Statistical analysis revealed significant interaction effects between machining parameters ($p = 0.0102$), indicating that spindle speed and feed rate should be selected synergistically to achieve favorable surface finish. Predictive models for Ra and Rq exhibited good agreement with the experimental results ($R^2 > 0.86$), with feed rate identified as the dominant factor influencing surface roughness.

From a practical perspective, the results indicate that robotic milling systems are capable of approaching the lower range of surface roughness typically reported for CNC machining under optimized conditions. Although robotic platforms do not match CNC machining in terms of consistency and overall precision, surface finish alone does not preclude the application of robotic milling in UHMWPE machining, particularly where flexibility, adaptability, and cost-effectiveness are prioritized.

This investigation focused exclusively on surface roughness under a constant depth of cut of 2 mm. Factors such as material removal rate, tool wear progression, depth-of-cut effects, dimensional accuracy, process repeatability, and robot dynamic behavior were not addressed and remain critical for a comprehensive feasibility assessment. Nevertheless, the present findings indicate that surface roughness is not a fundamental barrier to robotic machining of UHMWPE and provide an initial experimental basis for future, more comprehensive evaluations of robotic milling performance.

Acknowledgement

The authors would like to acknowledge the support of Universiti Teknologi Mara (UiTM), Cawangan Pulau Pinang, Malaysia, and Politeknik Tuanku Sultanah Bahiyah, Malaysia, for providing facility support for this research.

Conflict of Interest

The authors declare that they have no known financial or non-financial competing interests in any material discussed in this paper.

Author Contribution

The authors confirm contribution to the paper as follows: Wan Nor Shela Ezwane Wan Jusoh: ***conceptualization, methodology, formal analysis, writing -original draft, &*** *Validation. Mohamad Irwan Yahaya and Mahamad Hisyam Mahamad Basri:* ***supervision, data curation, investigation, writing -review & editing****. Shukri Zakaria and Md Razak Daud:* ***writing editing, visualization.***

Funding

This research is sponsored by the organization.

References

[1] C. James Ujam, "Adopting Manufacturing Flexibility to Achieve Competitive Advantage in a Global Economy," *International Journal of Multidisciplinary Research and Growth Evaluation*, 2025, [Online]. Available: www.allmultidisciplinaryjournal.com

[2] K. C. Yao, D. C. Chen, C. H. Pan, and C. L. Lin, "The Development Trends of Computer Numerical Control (CNC) Machine Tool Technology," *Mathematics*, vol. 12, no. 13, Jul. 2024, doi: 10.3390/math12131923.

[3] W. Liu, S. Zhang, J. Lin, Y. Xia, J. Wang, and Y. Sun, "Advancements in accuracy decline mechanisms and accuracy retention approaches of CNC machine tools: a review," *The International Journal of Advanced Manufacturing Technology*, vol. 121, no. 11, pp. 7087–7115, 2022, doi: 10.1007/s00170-022-09720-0.

[4] M. Makulavičius, S. Petkevičius, J. Rožėnė, A. Dzedzickis, and V. Bučinskas, "Industrial Robots in Mechanical Machining: Perspectives and Limitations," Dec. 01, 2023, *Multidisciplinary Digital Publishing Institute (MDPI)*. doi: https://doi.org/10.3390/robotics12060160.

[5] C. Urrea and J. Kern, "Recent Advances and Challenges in Industrial Robotics: A Systematic Review of Technological Trends and Emerging Applications," Mar. 01, 2025, *Multidisciplinary Digital Publishing Institute (MDPI)*. doi: 10.3390/pr13030832.

[6] M. Valente, I. Rossitti, I. Biblioteca, and M. Sambucci, "Thermoplastic Composite Materials Approach for More Circular Components: From Monomer to In Situ Polymerization, a Review," May 01, 2022, *MDPI*. doi: 10.3390/jcs6050132.

[7] Y. Qiao, L. D. Fring, M. R. Pallaka, and K. L. Simmons, "A review of the fabrication methods and mechanical behavior of continuous thermoplastic polymer fiber–thermoplastic polymer matrix composites," Feb. 01, 2023, *John Wiley and Sons Inc*. doi: 10.1002/pc.27139.

[8] K. Periasamy, E. Kandare, R. Das, M. Darouie, and A. A. Khatibi, "Interfacial Engineering Methods in Thermoplastic Composites: An Overview," Jan. 01, 2023, *MDPI*. doi: 10.3390/polym15020415.

[9] M. A. Samad, "Recent advances in uhmwpe/uhmwpe nanocomposite/uhmwpe hybrid nanocomposite polymer coatings for tribological applications: A comprehensive review," Feb. 02, 2021, *MDPI AG*. doi: 10.3390/polym13040608.

[10] Vidushi Sharma, Sheetal Chowdhury, Nandita Keshavan, and Bikramjit Basu, "Six decades of UHMWPE in reconstructive surgery," *International Materials Reviews*, vol. 68, no. 1, pp. 46–81, Jan. 2023, doi: 10.1080/09506608.2022.2047419.

[11] M. M. Rahman, M. A. S. Biswas, and K. N. Hoque, "Recent development on micro-texturing of UHMWPE surfaces for orthopedic bearings: A review," Sep. 01, 2022, *Elsevier Ltd*. doi: https://doi.org/10.1016/j.biotri.2022.100216.

[12] A. Bistolfi *et al.*, "Ultra-high molecular weight polyethylene (UHMWPE) for hip and knee arthroplasty: The present and the future," May 01, 2021, *Reed Elsevier India Pvt. Ltd.* doi: 10.1016/j.jor.2021.04.004.

[13] J. Sharath Kumar, R. Kumar, and R. Verma, "Surface Modification Aspects for Improving Biomedical Properties in Implants: A Review," *Acta Metallurgica Sinica (English Letters)*, vol. 37, no. 2, pp. 213–241, 2024, doi: 10.1007/s40195-023-01631-7.

[14] W. D. Lestari, A. T. Danaryanto, J. Jamari, A. P. Bayuseno, and A. Nugroho, "The Effect of The Machining Process UHMWPE on The Wear Behaviour of Acetabular Cups for Hip Implants," 2022.

[15] M. Piska and K. Urbancova, "Advanced Machining of Joint Implant UHMWPE Inserts," *Machines*, vol. 10, no. 11, Nov. 2022, doi: https://doi.org/10.3390/machines10111008.

[16] S. Dembski *et al.*, "Establishing and testing a robot-based platform to enable the automated production of nanoparticles in a flexible and modular way," *Sci. Rep.*, vol. 13, no. 1, Dec. 2023, doi: 10.1038/s41598-023-38535-6.

[17] S. Asif *et al.*, "Rapid and automated configuration of robot manufacturing cells," *Robot. Comput. Integr. Manuf.*, vol. 92, Apr. 2025, doi: 10.1016/j.rcim.2024.102862.

[18] R. C. Joshi, J. K. Rai, R. Burget, and M. K. Dutta, "Optimized inverse kinematics modeling and joint angle prediction for six-degree-of-freedom anthropomorphic robots with Explainable AI," *ISA Trans.*, Feb. 2024, doi: 10.1016/j.isatra.2024.12.008.

[19] M. A. Sofuoğlu and S. Gürgen, "Optimization of micromachining operation for particle reinforced UHMWPE composites," *Archives of Civil and Mechanical Engineering*, vol. 22, no. 3, p. 138, 2022, doi: 10.1007/s43452-022-00459-9.

[20] S. Hu *et al.*, "Temperature-influenced cutting mechanism of UHMWPE fibres," *J. Manuf. Process.*, vol. 113, pp. 183–196, Mar. 2024, doi: 10.1016/j.jmapro.2024.01.059.

[21] S. Hu, Y. Feng, X. Yin, X. Zou, and J. Qu, "Structure and properties of UHMWPE products strengthened and toughened by pulse vibration molding at low temperature," *Polymer (Guildf).*, vol. 229, Aug. 2021, doi: 10.1016/j.polymer.2021.124026.

[22] Budi Basuki and Andhi Akhmad Ismail, "Effects of CNC Milling Machining Parameters on the Surface Roughness of UHMWPE Biomaterial," *Int. J. Res. Eng. Technol.*, vol. 07, no. 10, pp. 68–73, Oct. 2018, doi: https://doi.org/10.15623/ijret.2018.0710011.

[23] W. D. Lestari, P. W. Anggoro, R. Ismail, J. Jamari, and A. P. Bayuseno, "Optimization of CNC Milling Parameters through the Taguchi and RSM Methods for Surface Roughness of UHMWPE Acetabular Cup," *International Journal of Mechanical Engineering and Technology (IJMET)*, vol. 10, no. 2, pp. 1762–1775, 2019.

[24] W. Wang, Q. Guo, Z. Yang, Y. Jiang, and J. Xu, "A state-of-the-art review on robotic milling of complex parts with high efficiency and precision," *Robot. Comput. Integr. Manuf.*, vol. 79, p. 102436, 2023, doi: https://doi.org/10.1016/j.rcim.2022.102436.

[25] D. K. Nguyen, H. C. Huang, and T. C. Feng, "Prediction of Thermal Deformation and Real-Time Error Compensation of a CNC Milling Machine in Cutting Processes," *Machines*, vol. 11, no. 2, Feb. 2023, doi: 10.3390/machines11020248.

[26] J. M. Wambua, F. M. Mwema, B. Tanya, and T. C. Jen, "CNC Milling of Medical-Grade PMMA: Optimization of Material Removal Rate and Surface Roughness," *International Journal of Manufacturing, Materials, and Mechanical Engineering*, vol. 12, no. 1, 2022, doi: 10.4018/IJMMME.293226.

[27] I. Beşliu-Băncescu, I. Tamaşag, and L. Slătineanu, "The influence of the machining strategy on milling of polyetheretherketone (PEEK)," *The International Journal of Advanced Manufacturing Technology*, vol. 132, no. 5, pp. 2773–2785, 2024, doi: https://doi.org/10.1007/s00170-024-13544-5.

[28] W. Lestari, L. Edahwati, T. Sari, N. Adyono, and N. Karaman, "SEM analysis of UHMWPE for biomedical application," *Biomedical and Mechanical Engineering Journal (BIOMEJ)*, vol. 1, no. 1, p. 5, 2021, doi: 10.33005/biomej. v1i1.23.

[29] W. N. S. E. Wan Jusoh, M. I. Yahaya, S. Zakaria, M. H. Mahamd Basri, M. R. Daud, and N. I. Ismail, "New approach to minimise surface roughness in Polytetrafluoroethylene (PTFE) through robotic spindle speed control," *ESTEEM Academic Journal*, vol. 21, no. March, pp. 106–118, Mar. 2025, doi: https://doi.org/10.24191/esteem.v21iMarch.4359.g3122.

[30] W. N. S. E. Wan Jusoh, M. I. Yahaya, S. Zakaria, M. H. Mahamad Basri, M. R. Daud, and N. I. Ismail, "Simulation-driven in robotic milling of soft material: Evaluating parallel and equidistant toolpath strategies using SprutCAM," *Academic Journal (EAJ) ESTEEM Academic Journal*, vol. 22, pp. 64–80, 2025, doi: https://doi.org/10.24191/esteem.v21iSeptember.6483.g4961.